Mixed cyclic trimers of porphyrins and dioxoporphyrins: geometry *vs.* electronics in ligand recognition

Zöe Clyde-Watson, Nick Bampos and Jeremy K. M. Sanders*

Cambridge Centre for Molecular Recognition, University Chemical Laboratory, Lensfield Road, Cambridge CB2 1EW, UK

NJC Letter

A series of metalloporphyrin-containing cyclic hosts has been prepared, which are electronically and geometrically programmed to recognize guests in a particular configuration. Electronic control is achieved by substituting the C—H *meso* positions with carbonyl groups, while geometric control is possible in the choice of the length of the rigid acetylene porphyrin linkers.

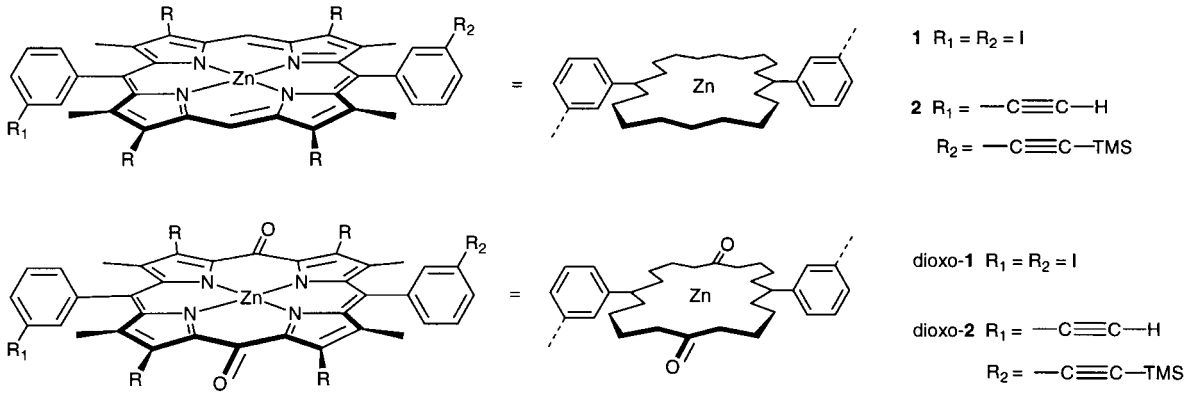

We describe here a new series of cyclic porphyrin oligomers containing a mixture of monomer units with different individual binding and structural properties; these oligomers address new questions about ligand preferences and dynamics within a host cavity. Previously we reported the convergent synthesis of an unsymmetrical porphyrin trimer[1] that has been used to change the stereochemical outcome of a Diels–Alder reaction.[2] This convergent approach allows access to a much more diverse array of host molecules than the one-pot Glaser–Hay coupling route to symmetrical trimers.[3–5] We describe here trimers containing electron-deficient dioxoporphyrin units in combination with standard porphyrins. Studying ligand orientation within these hosts allows us to assess the relative importance of *electronic* and *geometric* factors in intra-cavity binding.

The key features of the synthesis involve the palladium-catalysed cross-coupling[6] of a central diiodo porphyrin fragment **1** with two equivalents of a mono-alkyne porphyrin fragment **2** (Scheme 1). The resulting linear trimer **3a** is then deprotected and cyclized to give trimer **4** *via* an intramolecular Glaser–Hay coupling reaction, with the aid of an *s*-tri(4-pyridyl)triazine (Py_3T) template.[4,5] Modification of either the diiodo porphyrin or the monoalkyne porphyrin by oxidation before coupling leads to the mixed trimers.

Dioxoporphyrins[7] are more electron deficient than standard porphyrins and thus show an increased affinity for pyridyl ligands.[8] Furthermore, interruption of the conjugated system by the oxo functionalities divides the dioxo porphyrin into two separate dipyrromethane units, leading to the loss of conventional NMR ring current.[9] Conversions of porphyrins to their dioxo analogues were carried out efficiently using thallium trifluoroacetate in CH_2Cl_2–THF (3 : 1) followed by a sodium sulfite quench.[8] The mono-dioxo linear trimer was formed in 60% yield from the dioxo-diiodo porphyrin fragment, dioxo-**1**, and the monoalkyne porphyrin fragment **2**. Subsequent deprotection with TBAF (86%) followed by intramolecular coupling with the Py_3T template gave trimer mono-dioxo-**4**·Py_3T complex in 32% yield. A similar sequence gave bis-dioxo-**4**·Py_3T in an overall yield of 12% from monomers.

The ^1H NMR spectra of the 1 : 1 Py_3T complexes of trimers mono-dioxo-**4** and bis-dioxo-**4** show sharp and well-resolved resonances. Two-dimensional NMR experiments were employed to characterize the hosts and to investigate the mode of binding within the cavities. In the ^1H NMR spectrum of the 1 : 1 mono-dioxo-**4**·Py_3T complex, the pyridyl protons of the bound ligand are split in a ratio of 2 : 1, as predicted for a symmetrical tridentate ligand binding strongly to a host with C_2 symmetry. Well-resolved doublets (J = *ca.* 5 Hz) are observed at 2.17 ($H_{\alpha 2}$) and 6.23 ($H_{\beta 2}$) ppm, corresponding to the two pyridyl arms binding to standard porphyrins, while the pyridyl arm binding to the dioxoporphyrin gives rise to downfield doublets (J = *ca.* 5 Hz) at 8.86 ($H_{\alpha 1}$) and 7.91 ($H_{\beta 1}$) ppm [Fig. 1(*a*)].

The ROESY spectrum of this complex shows nOe contacts between the H_α protons of the Py_3T and the H_2 aromatic protons of the host that are directed into the cavity. The asymmetry of the complex results in three distinct subsets of

* E-mail: jkms@cam.ac.uk

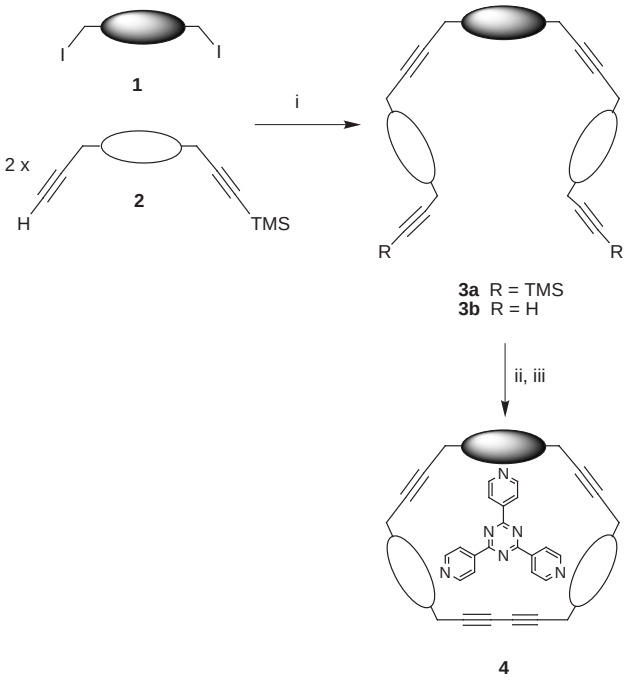

Scheme 1 (*i*) Cat. $Pd_2(dba)_3$, Ph_3As, Et_3N, THF, 35 °C; (*ii*) TBAF; (*iii*) Py_3T, CuCl, TMEDA, CH_2Cl_2

aromatic protons, which are assigned with the aid of the COSY spectrum. Exchange peaks are not observed in the ROESY spectrum between resonances of the bound ligand, indicating that once bound inside the cavity, the tridentate ligand is tightly anchored on the exchange (T_1) timescale. The corresponding spectra for the bis-dioxo-**4** · Py_3T complex are similar in appearance, but with the pyridyl protons split in a reversed 1 : 2 ratio [Fig. 1(*b*)].

Addition of one equivalent of the bidentate 4′-phenyl-4,2′ : 6′,4″-terpyridyl (Py_2Py)[10] ligand to mono-dioxo-**4** leads to more than one possible binding orientation inside the cavity. Due to the chelate effect, the ligand will preferentially bind to the interior face of the host, but the two pyridyl arms may bind either to the dioxoporphyrin and one of the two standard porphyrins, or to both porphyrin units. As dioxoporphyrin monomers bind pyridyl ligands more strongly than standard porphyrins,[11] one would expect the ligand to orientate itself asymmetrically within the host, between the dioxoporphyrin and one of the other porphyrins across an acetylene linker, rather than between two porphyrins across the butadiyne linker [Fig. 2(*a*)].

^1H NMR spectroscopy confirms this expectation, showing significant upfield shifts for the phenyl protons pointing towards a porphyrin unit (4.42, 4.96 and 6.00 ppm), the porphyrin-bound pyridyl protons (1.95 and 5.81 ppm for $H_{\alpha 2}$ and $H_{\beta 2}$, respectively) and the pyridyl protons bound to a dioxoporphyrin (8.12 and 7.29 ppm for $H_{\alpha 1}$ and $H_{\beta 1}$, respectively). Exchange peaks are observed in the ROESY spectrum between the $H_{\alpha 1}$ and $H_{\alpha 2}$ protons, the $H_{\beta 1}$ and $H_{\beta 2}$ protons and also between the two σ protons of the ligand, indicating ligand rotation within the cavity; two-point binding inside a host with three possible binding sites is not sufficient to anchor the ligand in a single orientation. As the two porphyrin units in the host are equivalent, ligand rotation about the C_2 dioxo axis is also possible, with one pyridyl arm binding to the dioxo unit while the other flips between the two remaining porphyrin units. This motion though, is too rapid to be detected on the chemical shift timescale, and only the average chemical shifts are recorded.

Addition of one equivalent of Py_2Py to a chloroform solution of bis-dioxo-**4** leads to a similar competitive binding process. The ligand may now bind to one dioxo unit and one

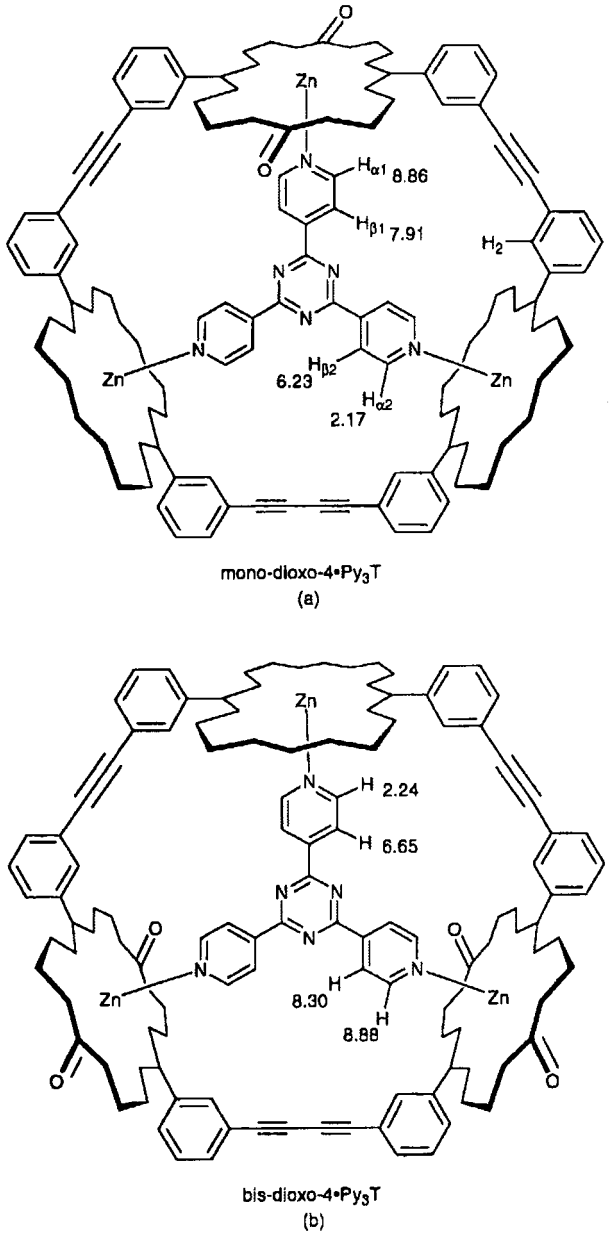

Fig. 1 Bound chemical shifts for Py_3T within trimer complexes

porphyrin across the shorter acetylene link, or instead may bind across the butadiyne link to both dioxounits, driven by the higher intrinsic binding to the dioxoporphyrins. Modelling studies complemented by the binding behaviour of Py_3T-like ligands in the 1,1,1 and 1,1,2 trimers suggest that *geometrically*, Py_2Py will prefer to bind across the shorter acetylene linker.[1–4] However, due to the relative difference in binding affinities, there will be an *electronic* preference to bind across the butadiyne link to both dioxo units. Alternatively, it is feasible that the ligand exchanges between both configurations. NMR evidence though, shows the Py_2Py ligand adopting a single orientation within the cavity [Fig. 2(*b*)], with resonances at 6.18 and 2.11 ppm for the pyridyl binding to a standard porphyrin unit; the second pyridyl, binding to a dioxo porphyrin, gives rise to signals at 8.66 and 7.85 ppm. If the ligand was binding to both dioxo units, the phenyl group would point into the shielding region of the porphyrin and upfield shifts would be expected for these protons, as observed for Py_2Py binding in mono-dioxo-**4**. As no other signals are observed in the region between 4.5 and 7.0 ppm, it seems that geometrical factors are dominant in determining the ligand orientation for this complex.

The increased affinity of Py_3T for the mixed dioxo trimers

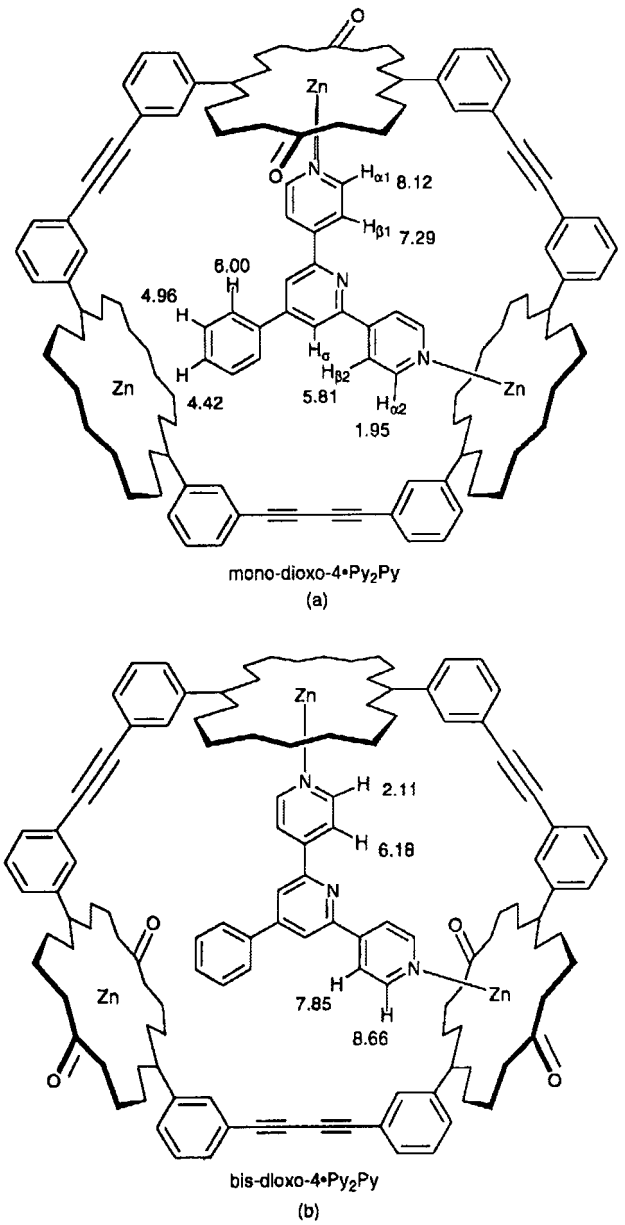

Fig. 2 Bound chemical shifts for Py_2Py within trimer complexes

was investigated more quantitatively by a series of ^{1}H NMR competitive binding experiments. Addition of one equivalent of mono-dioxo-**4** to a solution of the standard 1,1,2-trimer–Py_3T complex results in significant ligand transfer to the more electron deficient cavity ($K_{\text{mono-dioxo-4}}/K_{\text{1,1,2-trimer}} \approx 9$) with an estimated dissociation rate of $\approx 1 \times 10^{-4}$ s^{-1}. A dissociation rate of similar magnitude is observed for the transfer of Py_3T from mono-dioxo-**4** to bis-dioxo-**4** and $K_{\text{bis-dioxo-4}}/K_{\text{mono-dioxo-4}}$ is ≈ 9. Surprisingly, the transfer of Py_3T from the 1,1,2-trimer to bis-dioxo-**4** is so much faster that a reliable estimate of the dissociation rate is no longer possible. This striking discrepancy in ligand dissociation rates suggests an associative mechanism involving intermediates in which the ligand is bound simultaneously to both the original and competing host molecules:[12] the rate of transfer depends on the *difference* between the number of dioxo units in the two competing hosts.

In summary, the synthetic strategy of the 1,1,2 system allows easy access to a wide range of unsymmetrical cyclic hosts in which the electronic and geometric properties may be fine-tuned to influence and probe intra-cavity binding. Elsewhere we describe the ability of these trimers to accelerate a hetero Diels–Alder reaction.[13]

Experimental

Chemical shifts are quoted relative to residual solvent (7.25 ppm for ^{1}H and 77.0 ppm for ^{13}C) and coupling constants are given in Hz. All spectra were acquired at room temperature. Distilled solvents were used throughout. The final purification step in the preparation of the various porphyrins was crystallization by layered addition of hexane to a dichloromethane solution of the compound, followed by drying *in vacuo*.

Dioxo-diiodo porphyrin monomer (dioxo-1)

Thallium(III) trifluoroacetate (376 mg, 0.69 mmol) in dry CH_2Cl_2 (40 ml) was added dropwise to a solution of the diiodo porphyrin monomer (200 mg, 0.17 mmol) in CH_2Cl_2–THF (60 ml : 20 ml) at 0 °C over a period of 15 min. The mixture was stirred for a further 90 min before allowing to warm up to room temperature and then washing with aqueous sodium sulfite solution (0.25 M, 2 × 150 ml) followed by water (2 × 150 ml). The organic phase was dried ($MgSO_4$), filtered and evaporated to give a dark brown solid. Column chromatography on silica, eluting with 1 : 1 hexane–ethyl acetate, followed by recrystallization from CH_2Cl_2–hexane yielded 139 mg of pure dioxo-diiodo porphyrin dioxo-**1** (68%). ^{1}H NMR (250 MHz, $CDCl_3$): δ = 1.17 (s, 12H, Me), 2.45 (t, J = 7.7, 8H, CH_2), 2.86 (t, J = 7.7, 8H, CH_2), 3.59 (s, 12H, MeO), 7.18 (d, J = 4.9, 2H, aromatic H), 7.55 (s, 2H, aromatic H), 7.82 (t, J = 4.9, 2H, aromatic H); ^{13}C NMR (62.5 MHz, $CDCl_3$): δ = 12.67 (4 Me), 21.00 (4 CH_2), 34.33 (4 CH_2), 51.75 (4 MeO), 94.39 (2 aromatic C—I), 128.79, 130.63, 138.16, 138.49, (8 aromatic C—H), 136.18, 140.99, 141.51, 143.95, 151.41, 154.98 (20 quaternary aromatic and pyrrolic carbons), 174.46 (4 C=O ester), 182.13 (2 C=O dioxo); FAB-MS: calcd for $C_{52}H_{48}I_2O_{10}N_4Zn$ 1208.2, found 1207 $[M]^+$, 1229 $[M + Na]^+$; $\lambda_{max}(CH_2Cl_2)$/nm: 280.4, 343.8, 471.3, 566.4.

TMS-protected linear trimer (mono-dioxo-3a)

Dioxo-diiodo porphyrin dioxo-**1** (40 mg, 0.033 mmol) and mono-TMS porphyrin **2** (73 mg, 0.070 mmol, 2.1 equiv) in tetrahydrofuran–triethylamine (20 ml : 5 ml) were degassed (2 freeze–thaw cycles) and heated to 35 °C under argon. Triphenylarsine (24 mg, 0.079 mmol) and tris(dibenzylidene acetone)dipalladium(0) (9 mg, 9.85 mmol) were added and the mixture flushed through with argon for 5 min. The mixture was heated at 35 °C for 90 min before removal of the solvent by rotary evaporation to give a red solid. This was chromatographed on silica, eluting initially with hexane–ethyl acetate–chloroform (2 : 1 : 1 v/v) to remove any monomers, followed by neat chloroform to remove the product that appeared as a red-orange band. Recrystallization from dichloromethane–hexane yielded 60 mg of pure product (60%). ^{1}H NMR (250 MHz, $CDCl_3$): δ = 0.26 (s, 18H, TMS Me), 1.19 (s, 12H, dioxo Me), 2.37 (m, 8H, dioxo CH_2), 2.46, 2.49 (s, 24H, porphyrin Me), 2.82 (m, 8H, dioxo CH_2), 3.00, 3.01 (m, 16H, porphyrin CH_2), 3.65 (s, 12H, dioxo MeO), 3.52, 3.58 (s, 24H, porphyrin MeO), 4.22 (m, 16H, porphyrin CH_2), 7.11–8.26 (m, 24H, aryl H), 10.07 (s, 4H, *meso* H); ^{13}C NMR (62.5 MHz, $CDCl_3$): δ = 0.03 (TMS, 6 Me), 12.65, 14.19 (12 Me), 20.81, 21.76, 29.75, 34.23, 36.93 (24 CH_2), 51.72 (12 MeO), 89.03, 90.94, 94.66 (6 alkyne C), 97.17 (4 *meso* C—H), 105.07 (2 alkyne C—TMS), 127.68, 127.93, 128.51, 129.00, 129.33, 131.99, 132.00, 133.15, 135.99 (24 aromatic C—H), 118.45, 118.63, 122.28, 122.66, 124.22, 136.21, 138.77, 138.99, 139.76, 141.35, 143.39, 143.67, 144.18, 145.81, 147.52, 152.24 (66 quaternary aromatic and pyrrolic carbons), 173.57, 174.31 (12 C=O ester), 182.43 (2 C=O dioxo); FAB-MS: calcd for $C_{170}H_{166}N_{12}O_{26}Zn_3Si_2$ 3045.5572, found 3046 $[M]^+$, 1523 $[M]^{2+}$; $\lambda_{max}(CH_2Cl_2)$/nm: 345.7, 411.5, 469.8, 539.1, 571.6.

Mono-dioxo-4 · Py_3T complex

Py_3T[14] (4.8 mg, 0.0154 mmol) was added to a solution of the deprotected linear trimer mono-dioxo-**3b** (34 mg, 0.012 mmol) in dry CH_2Cl_2 (55 ml) and the mixture stirred at room temperature for 5 min under dry air before the addition of freshly prepared copper(I) chloride[15] (80 mg, 0.81 mmol, 70 equiv) and TMEDA (125 μl, 0.81 mmol, 70 equiv). Stirring was continued in the dark for 15 h after which the mixture was washed with water (6 × 50 ml), dried ($MgSO_4$), filtered and the solvent removed under reduced pressure to give a red-brown solid. Chromatography on silica, eluting with 2 : 1 : 1 $CHCl_3$–EtOAc–hexane allowed separation of the product from baseline material. Recrystallization from CH_2Cl_2–hexane yielded 12 mg of mono-dioxo-**4** · Py_3T complex (32%). ^1H NMR (500 MHz, $CDCl_3$): δ = 1.11 (s, 12H, dioxo Me), 2.17 (d, J = 5.6, 4H, $H_{\alpha 2}$, bound Py_3T), 2.25 (t, J = 7.0, 8H, dioxo CH_2), 2.50 (s, 24H, porphyrin Me), 2.74 (t, J = 7.0, 8H, dioxo CH_2), 3.02 (m, 16H, porphyrin CH_2), 3.41 (s, 24H, porphyrin MeO), 3.51 (s, 12H, dioxo MeO), 4.19 (m, 16H, porphyrin CH_2), 6.23 (d, J = 5.6, 4H, $H_{\beta 2}$, bound Py_3T), 7.19 (d, J = 7.8, 2H, H4), 7.38 (s, 2H, H2′), 7.50 (t, J = 7.8, 2H, H5), 7.79–7.81 (m, 6H, H6, H5′, H5″), 7.91 (d, J = 4.5, 2H, $H_{\beta 1}$, bound Py_3T), 8.03 (m, 4H, H4′, H4″), 8.14, 8.20 (2 d, J = 6.8, 4H, H6′, H6″), 8.31, 8.37 (2 s, 4H, H2′, H2′), 8.86 (d, J = 4.5, 2H, $H_{\alpha 1}$, bound Py_3T), 9.93 (s, 4H, *meso* H); ^{13}C NMR (62.5 MHz, APT, $CDCl_3$): δ = 12.36, 15.36 (12 Me), 20.68, 33.85, 36.85 (24 CH_2), 50.71, 51.17 (12 MeO), 82.43, 88.70, 90.90, 93.68 (8 alkyne C), 96.90 (4 *meso* C—H), 127.70, 127.87, 129.25, 129.82, 130.94, 131.08, 131.72, 133.01, 133.54, 133.88, 135.62, 137.65 (24 aromatic C—H), 111.54, 117.53, 123.88, 129.73, 130.95, 131.19, 131.49, 131.57, 132.78, 133.32, 134.04, 135.39, 136.73, 136.88, 137.66, 138.06, 139.82, 141.01, 141.29, 146.96, 154.24 (66 quaternary aromatic and pyrrolic carbons), 173.35, 173.44 (12 C═O ester), 181.10 (2 C═O dioxo), 120.19, 123.13, 143.79, 148.38 (12 aromatic C—H, Py_3T), 120.05, 130.67, 168.33, 174.28 (6 quaternary carbons, Py_3T); FAB-MS: calcd for $C_{164}H_{148}N_{12}O_{26}Zn_3 \cdot C_{18}H_{12}N_6$ 3211.5, found 3213 $[M]^+$; $\lambda_{max}(CH_2Cl_2)$/nm: 289.5, 339.4, 418.4, 468.5, 550.6.

Acknowledgements

We thank the EPSRC for financial support and the EPSRC Mass Spectrometry Service (Swansea) for FAB mass spectra.

References

1 A. Vidal–Ferran, N. Bampos and J. K. M. Sanders, *Inorg. Chem.*, 1997, **36**, 6117.
2 Z. Clyde-Watson, A. Vidal-Ferran, L. J. Twyman, C. J. Walter, D. W. J. McCallien, S. Fanni, N. Bampos, R. S. Wylie and J. K. M. Sanders, *New J. Chem.*, 1998, **22**, 493.
3 S. Anderson, H. L. Anderson and J. K. M. Sanders, *J. Chem. Soc., Perkin Trans. 1*, 1995, 2247.
4 A. Vidal-Ferran, Z. Clyde-Watson, N. Bampos and J. K. M. Sanders, *J. Org. Chem.*, 1997, **62**, 240.
5 V. Marvaud, A. Vidal-Ferran, S. J. Webb and J. K. M. Sanders, *J. Chem. Soc., Dalton Trans.*, 1997, 985.
6 K. Sonogashira, Y. Tohda and N. Hagihara, *Tetrahedron Lett.*, 1975, 4467.
7 G. H. Barnett, B. Evans and K. M. Smith, *Tetrahedron*, 1975, **31**, 2711.
8 D. W. J. McCallien and J. K. M. Sanders, *J. Am. Chem. Soc.*, 1995, **117**, 6611.
9 E. D. Becker, R. B. Bradley and C. J. Watson, *J. Am. Chem. Soc.*, 1961, **83**, 3743.
10 F. Kröhnke, *Synthesis*, 1976, 1.
11 Due to the presence of a bound water molecule there is no shift in the Soret band of dioxo porphyrin monomers on binding pyridine-based ligands. Detailed studies of the Q-band region of the visible spectrum did not yield simple 1 : 1 titration curves and failed to reproduce very large earlier estimates[8] for the magnitude of these binding constants. However, the competition experiments described here do confirm that dioxo porphyrins bind more strongly than conventional porphyrins to pyridine ligands.
12 This is precedented in other porphyrin oligomers: C. A. Hunter, M. N. Meah and J. K. M. Sanders, *J. Am. Chem. Soc.*, 1990, **112**, 5773.
13 M. Marty, Z. Clyde-Watson, L. J. Twyman, M. Nakash and J. K. M. Sanders, *Chem. Commun.*, 1998, 2265.
14 H. Biedermann and K. Wichmann, *Naturforsch., B*, 1974, **29**, 360.
15 R. N. Keller and H. D. Wycoff, in *Inorganic Syntheses*, ed. W. C. Fernelius, McGraw-Hill, New York, 1946, vol. 2, p. 1.

Received in Montpellier, France, 13*th July* 1998;
Letter 8/05504A